Hindawi
Shock and Vibration
Volume 2020, Article ID 6467354, 12 pages
https://doi.org/10.1155/2020/6467354

Research Article

Effect of Welding Residual Stress on Along-Wind Fatigue Life of Welded Joints in Guyed Mast

Weilian Qu, Min Wang, and Qiang Zhou

Hubei Key Laboratory of Roadway Bridge and Structure Engineering, Wuhan University of Technology, Wuhan, Hubei 430070, China

Correspondence should be addressed to Weilian Qu; quweilian_wh@126.com

Received 13 June 2019; Revised 2 December 2019; Accepted 9 December 2019; Published 27 January 2020

Academic Editor: Dario Di Maio

Copyright © 2020 Weilian Qu et al. This is an open access article distributed under the Creative Commons Attribution License, which permits unrestricted use, distribution, and reproduction in any medium, provided the original work is properly cited.

On the premise of only considering along-wind effect on guyed mast, the influence of welding residual stress on the fatigue life of welded joints is evaluated in this paper. Since the sum of residual stress and along-wind-induced dynamic stress exceeds the yield strength of structural steel, the effect of residual stress relaxation is included in the numerical analysis. The multiscale finite element analysis of guyed mast is developed in order to capture accurately stress field distribution of welded joint for the "welding-wind-induced" case in which both residual stress and along-wind-induced stress are taken into consideration, and the stress response characteristics at fatigue critical point of welded joints are pointed out. It is found that the "welding-wind-induced" stress field of welded joint can be approximately considered as multiaxial proportional loading state and hence the stress-based von Mises criterion can be adopted to evaluate the fatigue life of welded joints. Based on the S-N curve of stress fatigue life for welded specimens with structural steel commonly used in guyed masts, the fatigue damage of key welded joints is predicted, and as a consequence, the influence of welding residual stress on the fatigue life of welded joints is discussed.

1. Introduction

Guyed mast is a kind of widely used wind-sensitive structure. Due to the characteristics of high flexibility and lightweight, welded joints of the guyed mast are vulnerable to long-term strong wind load, which may induce severe fatigue damage at weld seams. Therefore, there is great need to predict fatigue life of welded joints of such flexible steel structure.

In the field of fatigue life prediction of flexible structures under strong wind load, Wirsching and Shehata [1] proposed a design method for high-cycle fatigue according to the improved probability-based Palmgren–Miner (P-M) rule and rain-flow counting method. Peil and Telljohann [2] studied the fatigue life of flexible high-rise structures under wind loads. Tovo [3] analyzed the relation between fatigue damage assessment and counting method and proposed a new rain-flow damage assessment method, which can give satisfactory approximate fatigue damage prediction under combined wide- and narrow-band Gaussian loads. Repetto and Solari [4] assessed the wind-induced fatigue damage of several types of mast structures in both downwind and crosswind directions when the changes of wind speed and wind direction were considered. However, in these researches, the influence of residual stresses of welded joints on fatigue life is ignored. Horas et al. [5] proposed the application of modal superposition technique combined with elastoplastic analysis to evaluate the fatigue crack initiation of structural members. Based on the material damage-elastoplastic-coupled mechanical model, He et al. [6] used the continuous damage mechanics (CDM) module in the ABAQUS program to study fatigue performance of wind turbine gears caused by tolling contact. Ziegler et al. [7] analyzed fatigue crack growth at two structural hot spots by using a fracture mechanics model applying Paris' law and studied load sequence and weather seasonality influence fatigue crack growth for monopile-based offshore wind turbines. Lecheb et al. [8] investigated dynamic crack fatigue life of a 25 m length wind turbine blades and discussed the influence of displacement, strain, stress, and mode shapes on

crack growth. Wang and Soutis [9] studied fatigue performance of composite T joints used in wind turbine blades with various fibre reinforcement architectures and analyzed stress distribution and initiation and growth of a delaminating crack by developing a finite element model. Fang et al. [10] assessed wind-induced fatigue of large-scale complicated high-rise steel structure by using equivalent structural stress method and hot spot stress method as well as nominal stress method. Hosseiny and Jakobsen [11] used the submodel method to study the fatigue crack growth life of offshore wind turbine blades under wind force. Do et al. [12] estimated fatigue life of wind turbine tower bases throughout Colorado and discussed the effects of wind distribution and turbulence intensity. Shuang and Song [13] investigated crack initiation and growth life of wind turbine blades by using the linear cumulative damage theory and linear crack propagation theory and found that non-Gaussian characteristics of wind inflows had a noticeable influence on both extreme response and fatigue damage. Since it is very difficult to estimate the residual stress distribution along the crack path, as pointed out by Colombi and Doliński [14], in the previous research, the effect of welding residual stress on the fatigue life of welded joint welds was neglected.

Weld seams are weakness in fatigue life of welded joints of high-rise structures. Due to the difficulty in determining welding residual stress field of weld joint, the effect of residual stress on fatigue life of weld joint is so complicated that it is still not fully understood today. Hence, the influence of welding residual stress field is still questionable.

This paper presents a method to study the effect of welding residual stress on the fatigue life of welded joints of the guyed mast subjected to along-wind load. A multiscale finite element analysis method is proposed to calculate the "welding-wind-induced" stress of welded joints with the consideration of residual stress relaxation when welding residual stress is superimposed on wind-induced stress. As a comparison, the "wind-induced" stress of welded joints is also calculated neglecting welding residual stress. It is found that the three-dimensional stress field of welded joint can be approximately considered to be multiaxial proportional and so the stress-based von Mises criterion can be used to predict the fatigue life of welded joints. Then the welded specimens with structural steel commonly used in the guyed mast are tested to obtain the S-N curve of stress fatigue life, and the fatigue damage value of key welded joints is calculated based on the Miner linear cumulative fatigue damage model.

2. Multiscale Finite Element Analysis of Along-Wind "Welding-Wind-Induced" Stress of Welded Joints

2.1. Multiscale Finite Element Modeling of Along-Wind-Induced Stress of Welded Joints. The along-wind-induced response of guyed mast can be given by

$$[M]\{\ddot{X}\} + [C]\{\dot{X}\} + \{f\{X\}, t\} = \{P\{t\}\}, \quad (1)$$

where $[M]$, $[C]$, and $\{f\{X\}, t\}$ are the mass matrix, the damping matrix, and the restoring force vector respectively; $\{X\}$, $\{\dot{X}\}$, and $\{\ddot{X}\}$ are the horizontal displacement, velocity, and acceleration vectors of concentrated masses, respectively; and $\{P\{t\}\}$ is the wind load vector acting on the nodal layers where the lumped masses are concentrated.

The guyed mast structure is composed of beam and cable as well as welded gusset plate at the beam-cable connection. Under the action of wind, various structural components of the mast structure will produce different dynamic responses. In order to accurately obtain the along-wind-induced stress field of the welded joints, element types with different scales are used for different structural components. Due to the calculation ability limitation of the desktop computer, it is impossible to analyze precisely all the welded gusset plates and welds between cables and main structures. Only the most disadvantageous welded joints are modeled and analyzed in detail. Accordingly, the multiscale finite element model for guyed mast includes the following: (1) elastic beam element based on the meter scale, mainly used in truss element of the main structure; (2) strut element, based on the meter scale, mainly used for cable members; considering that the cable of the guyed mast will be pretensioned to ensure that the cable is always in tension state when wind-induced vibration occurs in guyed mast, the tensioned member element can be used; (3) elastic solid element, based on the centimeter scale, mainly used for welded gusset plates; (4) elastic-plastic solid element, based on the millimeter scale, mainly used for welds.

For the mast structure shown in Figure 1, the guyed mast is a steel lattice truss, which consists of steel tubular chords having a diameter Φ102/6 and steel tubular cross webs having diameter Φ54/4. The total height of the guyed mast is 152 m, and the cross section of the mast is a uniform equilateral triangle with each side having a length of 1.0 m. The lattice trussed mast is divided into 92 segments with each segment having a length of 1.25 m. Three gusset plates are welded to the chord at each vertex of the triangle at the height 55 m of the mast, and the other three gusset plates are welded to the chord each vertex of the triangle at the height 115 m of the mast as shown in Figure 1. Each gusset plate is connected to a guying cable. The projection length of the cables is 7.0 m, and the projection angle between any adjacent two cables at each layer is equal to 120°. All members of the mast are made of the Q35 steel with a modulus of elasticity of 2.0×10^{11} N/m^2, while the guying cables are made of a galvanized steel wire with a modulus of elasticity of 1.2×10^{11} N/m^2. The cables connecting the upper level of gusset plates have a diameter of 14.5 mm with a cross-sectional area of 2.688×10^{-4} m^2, while the cables connecting the lower level of joint plates have a diameter of 18.5 mm with a cross-sectional area of 1.65×10^{-4} m^2 (Figure 1). The structure of the welded joints between the cable and the mast is shown in Figure 2.

For this guyed mast structure, the commercial finite element program ANSYS is adopted to establish its multiscale finite element model, in which BEAM44 element with meter scale, LINK10 element with meter scale, SOLIID45 element with centimeter scale, and SOLIID95 element with millimeter scale are selected for beam, cable, gusset plates, and weld seams, respectively. The multiscale finite element model of the guyed mast is shown in Figure 3.

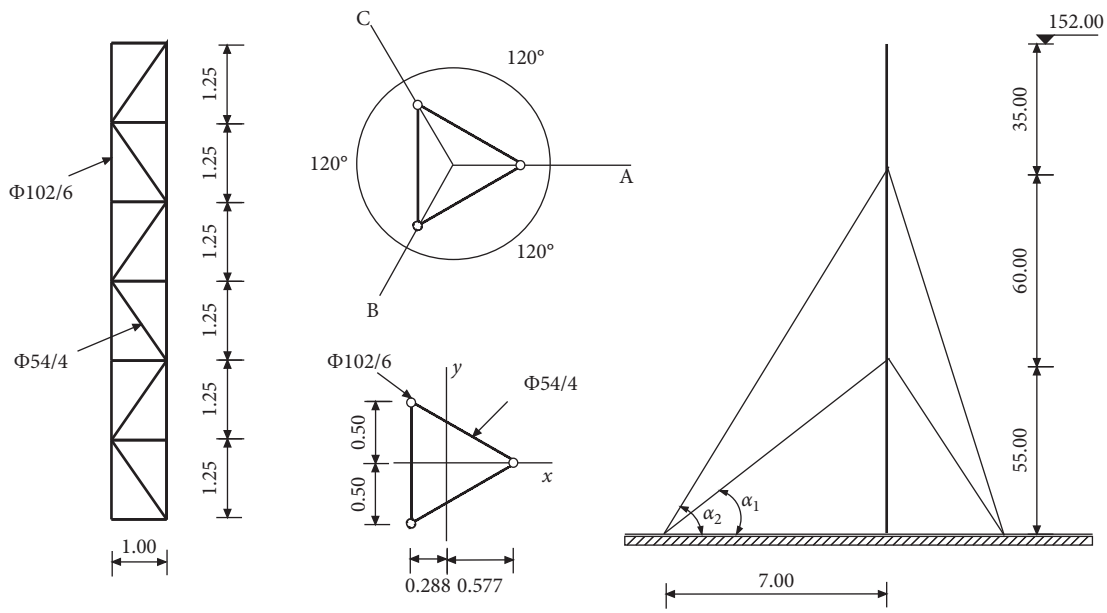

Figure 1: Schematic diagram of the guyed mast structure.

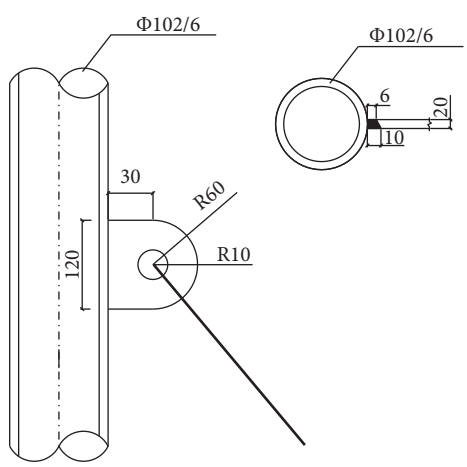

Figure 2: Schematic diagram of the welded joint.

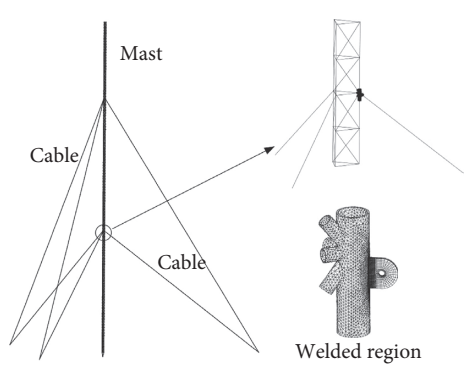

Figure 3: Multiscale finite element model of the guyed mast structure.

2.2. Finite Element Simulation of Residual Stress in Welded Joint. The residual stresses in welded joints can be simulated and calculated by ANSYS. Therefore, it is necessary to establish a common geometric model and element meshing model for both thermal analysis and thermoelastic-plastic analysis. The temperature field time history during welding process is obtained by thermal finite element analysis, and then the thermoelastic-plastic finite element analysis is carried out to obtain the residual stress field in the welded joint. The flowchart of finite element numerical simulation of welding process is shown in Figure 4.

For the welded joints of the guyed mast shown in Figure 2, considering the affected zone of welding residual stress and the connection requirement of elements with different types and different scales in the multiscale finite element model, the welded joint includes the welds seam, welded gusset plate, and the end parts of the chord and cross web connected to the joint plate as shown in Figure 5.

The fine mesh of welded joints is shown in Figure 6. In the finite element analysis of welding residual stress, SOLID70 and SOLIID90 elements are used for welding thermal analysis, and SOLID45 and SOLIID95 elements are used for welding thermal elastic-plastic analysis, respectively.

Since the welded joints are manually joined by the electrical arc welding method, the parameters for the Gaussian heat source are determined by the actual welding process parameters. The welding process is 10 seconds long and the simulation time step for the welding process is 0.2 seconds. The cooling process of the welds is 1090 seconds long consisting of three stages of 10 seconds, 30 seconds, and 1050 seconds, and the corresponding time steps are taken as 0.2 seconds, 1 second, and 10 seconds. Figures 7 and 8 demonstrate the distribution of the temperature field and the von Misses residual stress field in the welded joint at 1100 seconds, respectively. From Figure 8, it can be seen that the maximum equivalent residual stress is located at the top of the weld seams between the welded joint plate and the chord of the mast.

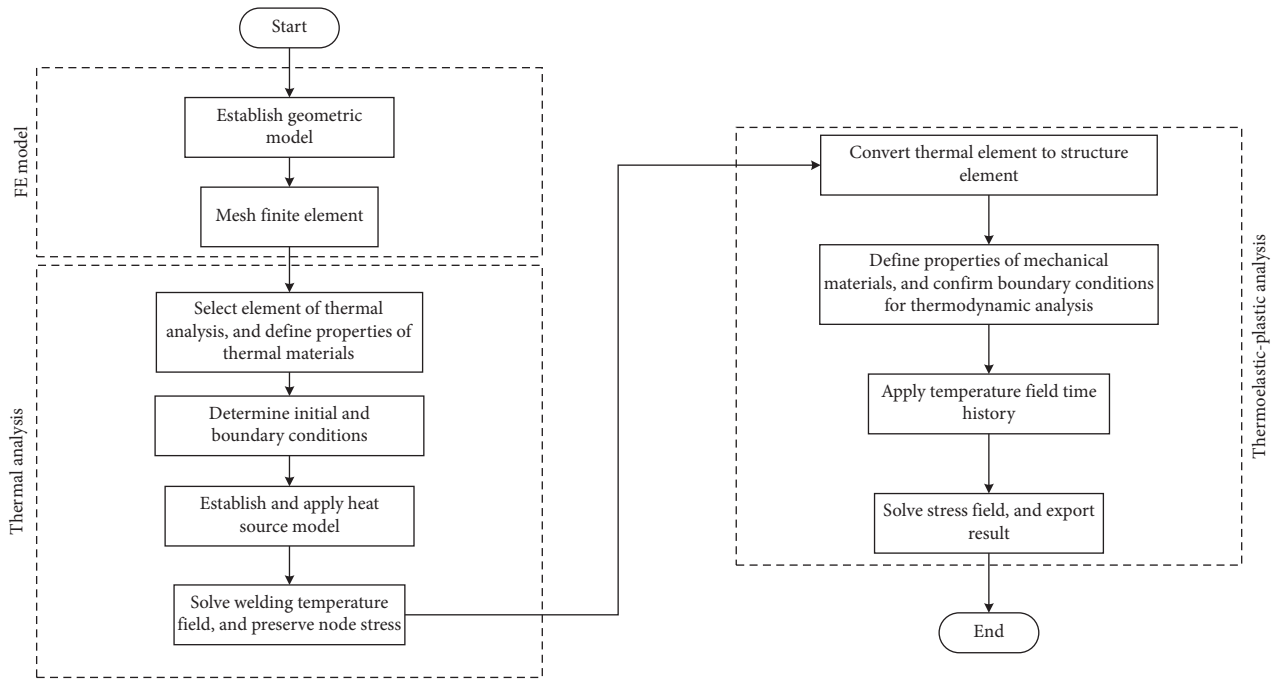

Figure 4: Flowchart of finite element analysis of welding process.

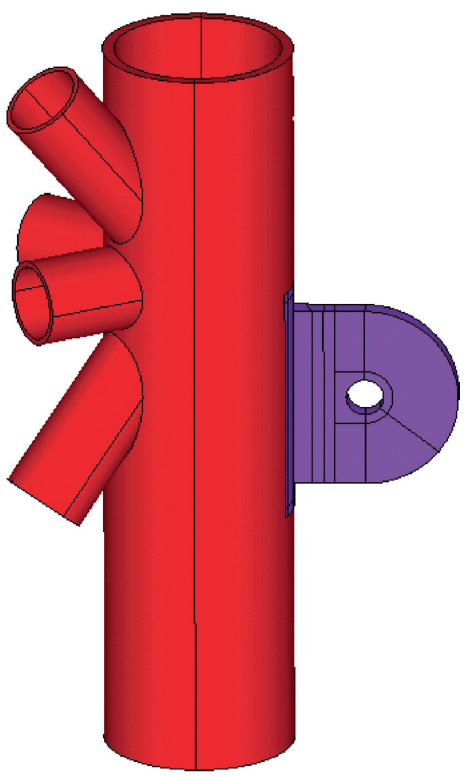

Figure 5: Geometric model of the welded joint.

2.3. Tests on Welding Residual Stress Relaxation. When the welding residual stress is applied to the wind-induced stress of welded joints, the residual stress will relax itself if the superimposition exceeds the yield strength of structural steel. In order to verify this fact, the experiments on welding residual stress relaxation are carried out.

The tested welding specimen is shown in Figure 9. The weld seam is along the longitudinal direction of the flat specimen, and the groove butt weld was adopted. External longitudinal tensile and compressive loads are applied to the specimen. Figure 10 shows the longitudinal welding residual stresses at the cross section of the welded specimens after one cycle under the cyclic stresses with the amplitude of 240 MPa, where the dotted line stands for the simple superposition of the longitudinal welding residual stresses and the amplitudes of longitudinal cyclic stresses, the black solid line is the curve of the longitudinal welding residual stresses curve, and the blue solid line is the measured stresses after relaxation of longitudinal welding residual stresses, which are the sum of the amplitudes of longitudinal cyclic stresses and the relaxed residual stresses. Figure 10 shows that when the sum of the maximum welding residual stresses and the amplitude of cyclic stresses exceeds the yield strength of the material leading to relaxation of the residual stresses under the cyclic load. At this time, the magnitude of welding residual stress will be significantly reduced.

2.4. "Welding-Wind-Induced" Stress Response of Welded Joint. Investigations of wind-induced collapses of steel guyed masts have shown that the wind loading often induces cyclic stresses at the welding zone in joint plates, where the residual stresses were induced during welding process. The combined action of the residual stresses and the cyclic stresses induced by the wind load may cause fatigue crack initiation and propagation at welds of gusset plates, which subsequently weakens the bearing capacity of the guyed mast and leads to its serious damage collapse and even to its collapse. Therefore, it is necessary to study whether the welding

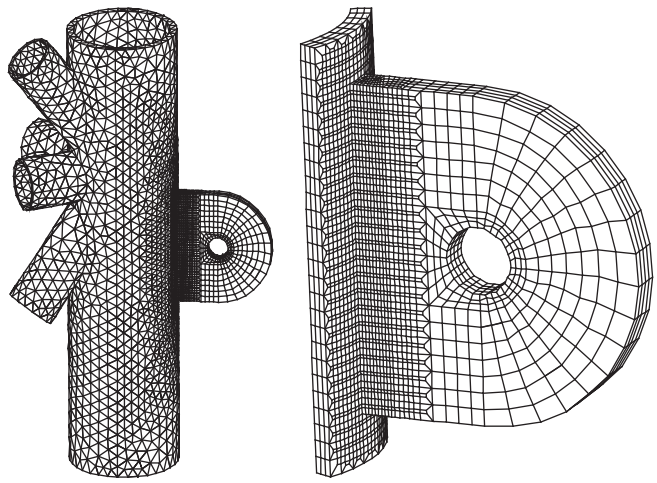

(a) (b)

Figure 6: Refined mesh model for welded joints. (a) Finite element model of welded joints. (b) Details of the gusset plate and weld.

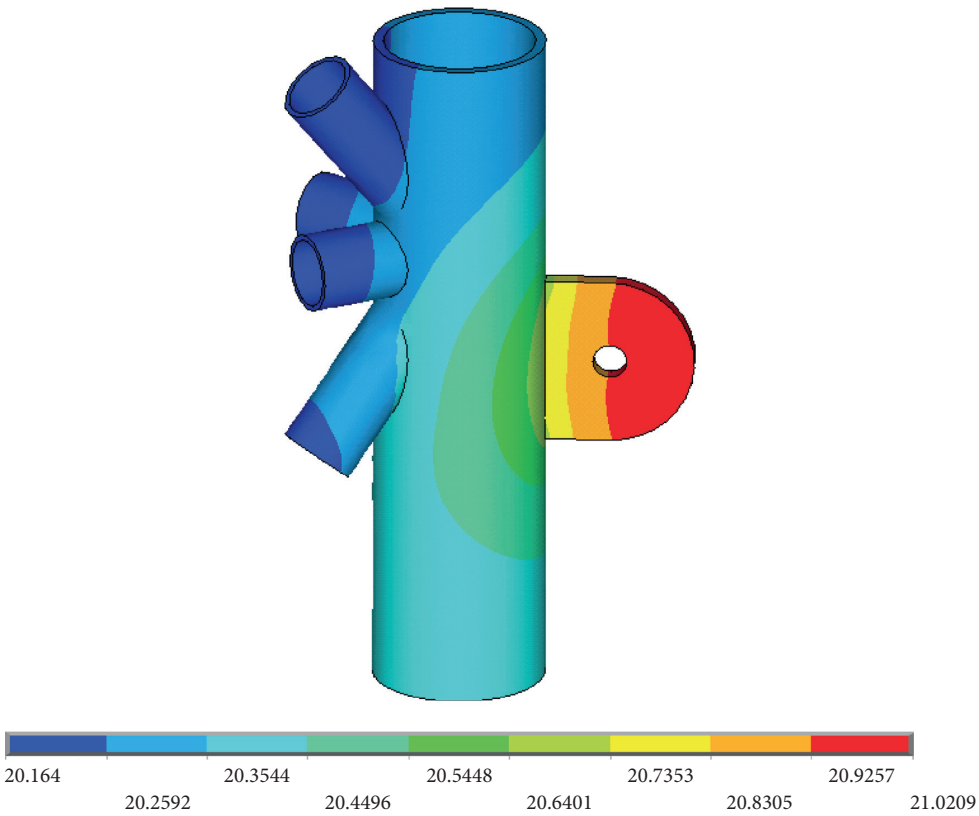

Figure 7: Distribution of the temperature field.

residual stresses increase the wind-induced stresses at the welds or have little effect.

It is well-known that the wind load is composed of the mean and fluctuating component, so the wind load acting on the guyed mast is obtained based on the average wind speed at the standard height and the ground roughness coefficient as well as the spatial correlation of wind field. The average wind speed at 10 m height of practical guyed mast is 22 m/s and site roughness coefficient is 0.16. The most unfavorable wind comes from the 0° direction. Based on the Davenport wind speed spectrum, the fluctuating wind speed samples are simulated by the linear filtering method, which is associated with the average winds to establish the time history of the wind load. The wind load acts on nodal layers where the lumped masses are concentrated.

Based on the residual stress field obtained from the welding thermal analysis and thermoelastic-plastic analysis, a multiscale finite element model as shown in Figure 3 is

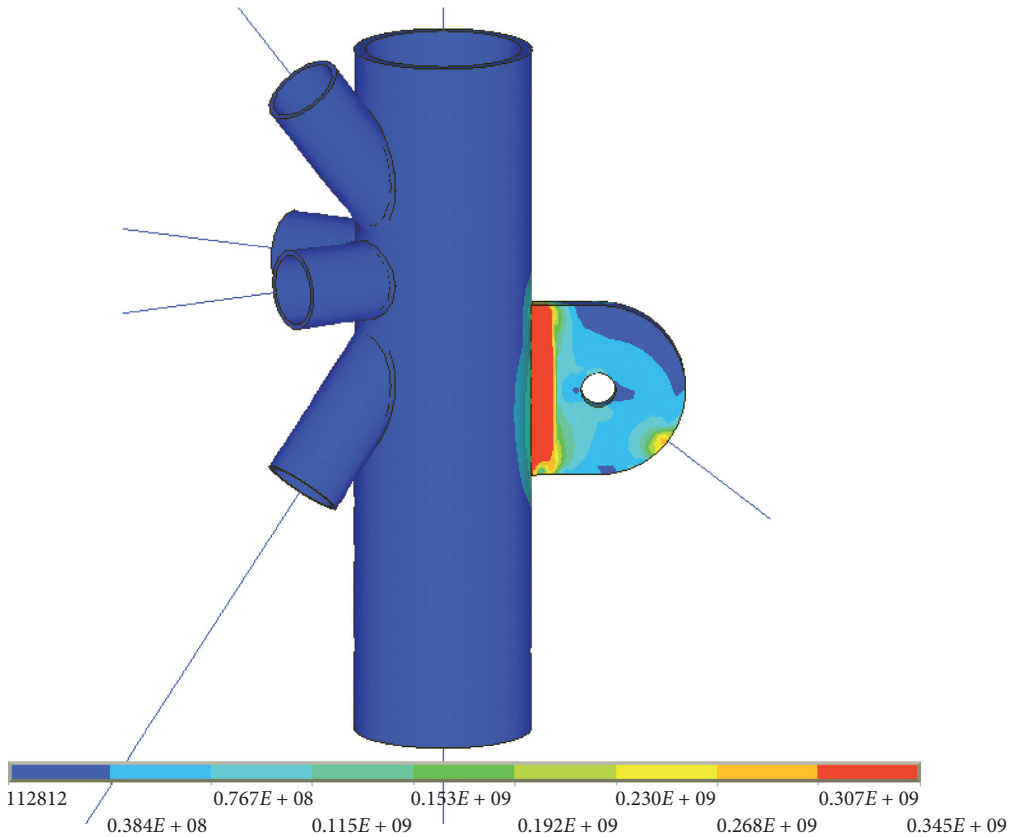

Figure 8: Distribution of von Misses residual stresses.

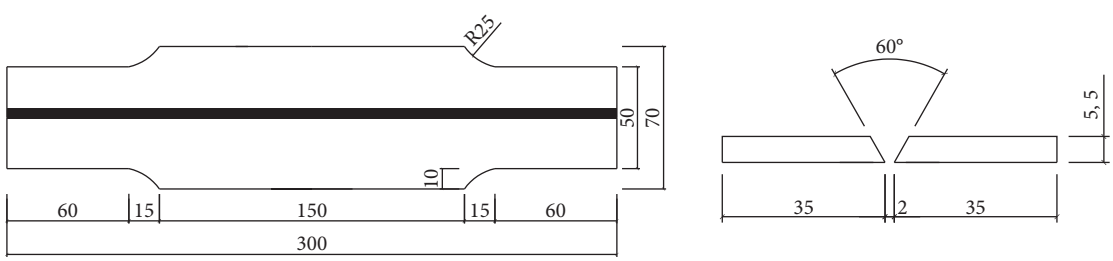

Figure 9: Welding specimen and groove size.

established for the "welding-wind-induced" response analysis of the guyed mast and welded joints. In the analysis, the residual stress field is treated as the initial stress field in the welded joints with property of self-equilibrium and relaxation. Finally, the top end of the weld between the welded gusset plate and the chord of the mast is considered as the fatigue critical position, and the along-wind-induced stress responses at the critical position with and without the consideration of welding residual stress are shown in Figure 11.

2.5. Proportional Loading Condition at Fatigue Critical Point of Welded Joint. In order to select a proper approach for fatigue life prediction of welded joints of the guyed mast under strong wind load, the primary task is to evaluate the three-dimensional stress state at the critical point, which may be produced either by proportional loading or by nonproportional loading. Based on multiaxial fatigue theory and experimental study [15–18], if the along-wind-induced three-dimensional stress state at the fatigue critical position of welded joint is proportional, the equivalent stress/strain approaches can give satisfactory estimation of the fatigue life.

Since the mechanism of fatigue damage caused by crack initiation for structural steel obey the metal crystal slip rule, it can be considered that the fatigue damage occurs on the maximum shear stress plane, which can be defined as the critical plane according to the multiaxial fatigue theory, at the fatigue danger point of the key welded joints [19, 20]. If the stress state of the fatigue danger point is proportional, the angle of the critical plane is constant, while if the stress state is nonproportional, the angle time history of the critical plane varies [15, 21].

When the guyed mast is subjected to the along-wind load, Figure 12 shows the time history of the maximum shear

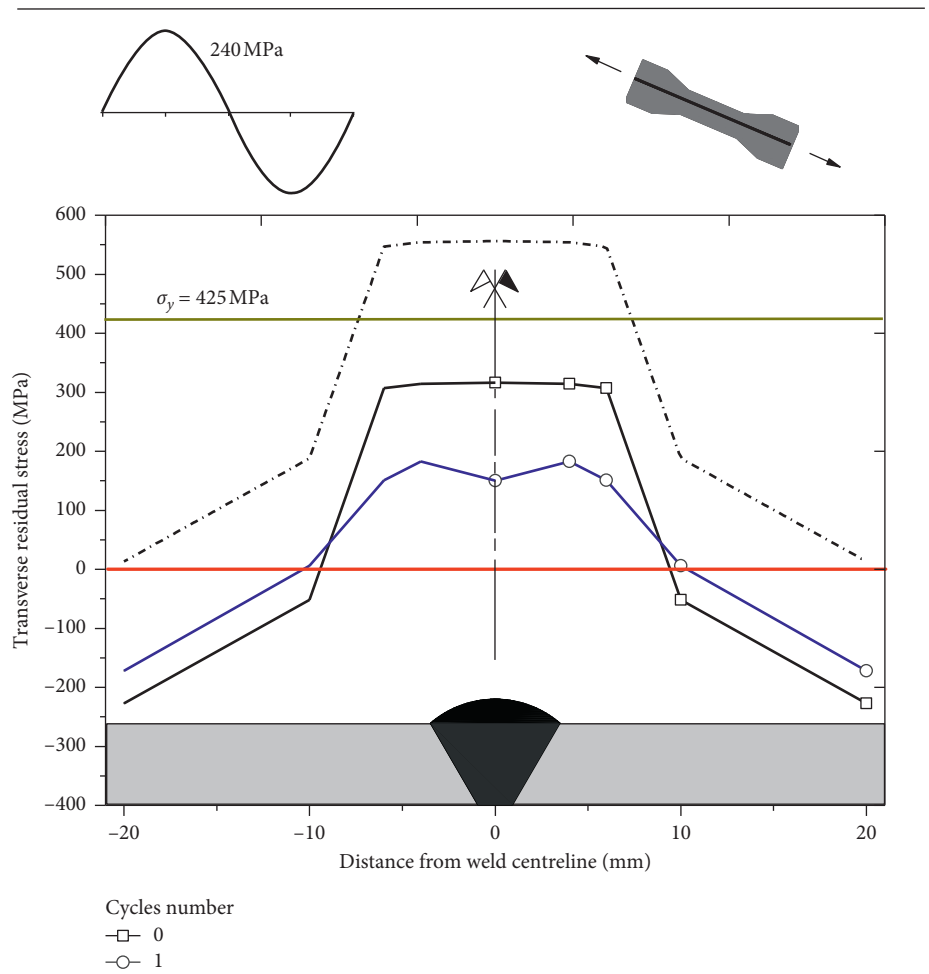

Figure 10: Effect of 240 MPa cyclic stress on residual stress relaxation in longitudinal welding.

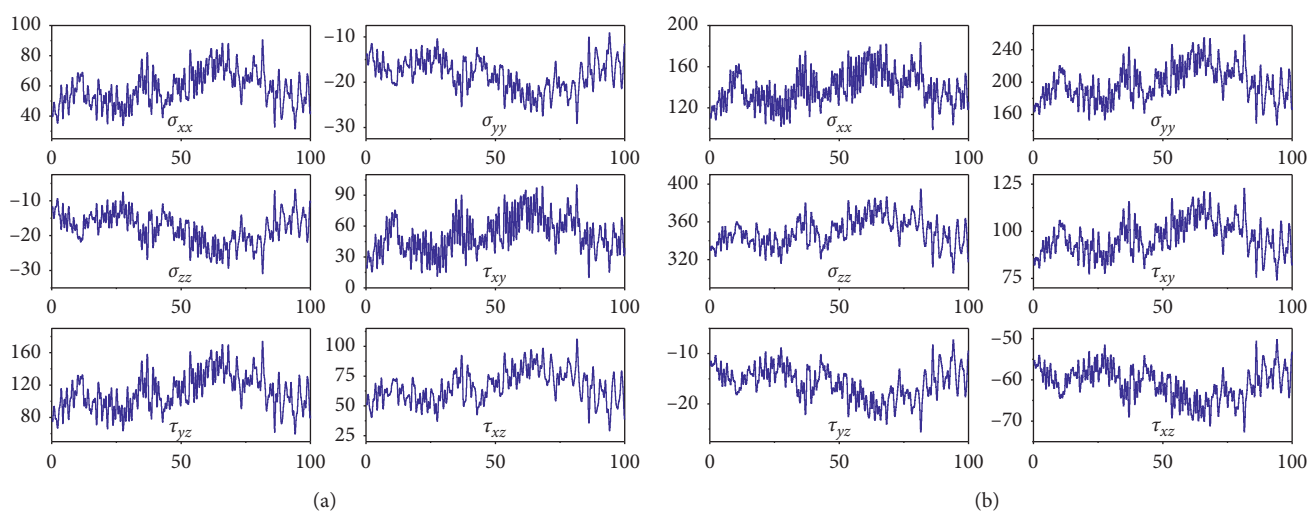

Figure 11: Multi-dimensional stress time history at the fatigue hazard point of key welded joint. (a) "Wind-induced" case. (b) "Welding-wind-induced" case.

stress plane position angle at the fatigue critical point of the welded joint without and with the consideration of welding residual stress. It can be seen that critical plane angle for the "wind-induced" case is a straight line parallel to the time axis and that for the "welding-wind-induced" case can be approximately considered as a line parallel to the time axis. The maximum shear stress plane of the former, i.e., the critical plane angle, is $\theta = 142^\circ$ and $\phi = 100^\circ$, while the latter is

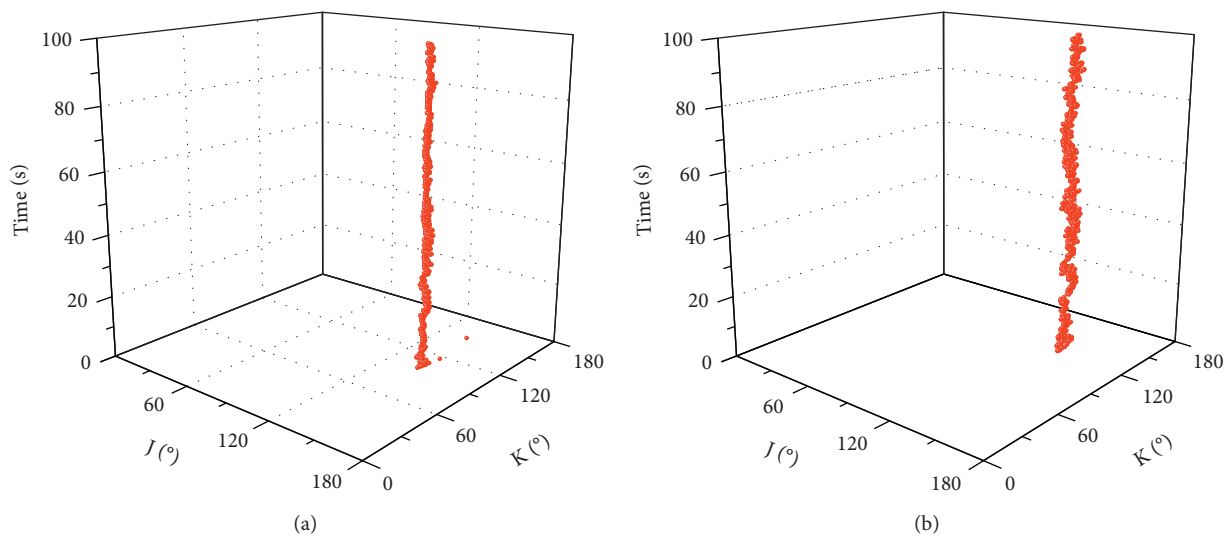

Figure 12: Time-varying angle of maximum shear stress at the fatigue critical point. (a) "Wind-induced" case. (b) "Welding-wind-induced" case.

approximately $\theta = 135^\circ$ and $\phi = 132^\circ$. So, it can be concluded that the stress state at the fatigue critical point is proportional for the "wind-induced" case and weak proportional for proportional for the "welding-wind-induced" case.

Furthermore, the wind-induced equivalent stresses of the welded joints are less than the yield stress of structural steel (Figure 13), and no plastic strain occurs at the welded joints when the guyed mast is subjected to along-wind loading. Therefore, the wind-induced fatigue of welded joints of the guyed mast can be approximately considered as multiaxial proportional high-cycle fatigue, and the fatigue crack initiation life of the welded joint can be predicted accurately by the equivalent stress method. In the following numerical analysis, the stress-based von Mises criterion, which is suitable for most metal material, is adopted.

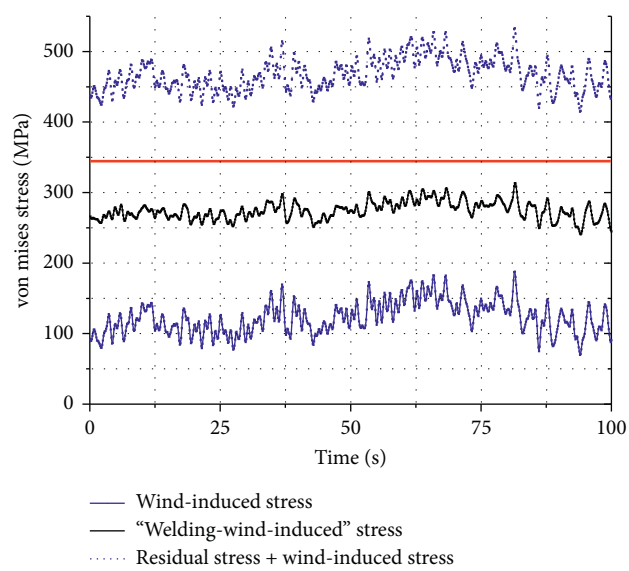

Figure 13: Comparison of stress time history at the fatigue critical point.

3. Test on S-N Curve of Stress Fatigue Life of Q345 Welded Specimens

In order to obtain the S-N curve of fatigue life of welded joints in the guyed mast, the uniaxial high-cycle fatigue test was carried out based on the Q345 structural steel groove butt weldment.

3.1. Welded Specimens and Test Equipment. In this paper, the dog bone plate welded tensile specimens shown in Figure 14 are used. The base material is Q345 structural steel. The fatigue specimens are sampled from the Q345 steel butt welding plate and machined to the designed shape and size, shown in Figure 14. The middle part of the specimens is the weld.

In order to ensure the full penetration of the weld root, the plate is prepolished and grooved. The groove shape and size conform to the requirements of GB T2651-2008. Multilayer welding is adopted until the size of the weld foot meets the requirements. After welding, the residual stress in the weldment is eliminated by overload treatment. Referring to the cyclic fatigue test method in GB15248-2008, the test was completed by electrohydraulic servo high-frequency fatigue testing machine (Shimadzu), as shown in Figure 15.

3.2. Scenarios and Test Results. From Figure 13, it can be seen that the stress amplitude of the equivalent stress history curves at the welding fatigue critical point is less than 200 MPa in most random cycles, so seven loading scenarios are designed, as shown in Table 1. Two specimens are tested under each loading condition.

In order to prevent the specimen from bending or warping during the test, the specimens are vertically installed in the center of the clamping fixture, as shown in Figure 16.

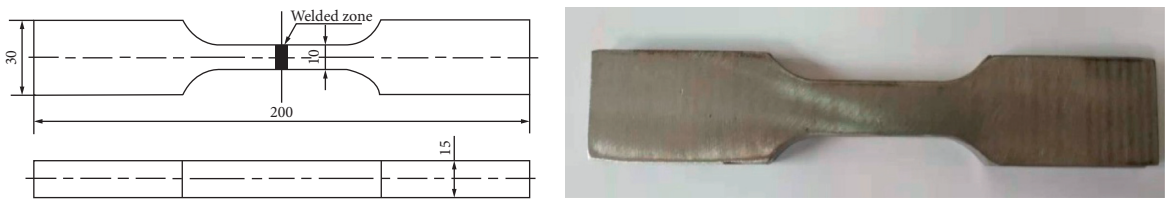

(a) (b)

Figure 14: Geometry of the welded steel specimen. (a) Geometry of the weldment (unit: mm). (b) Welded specimen.

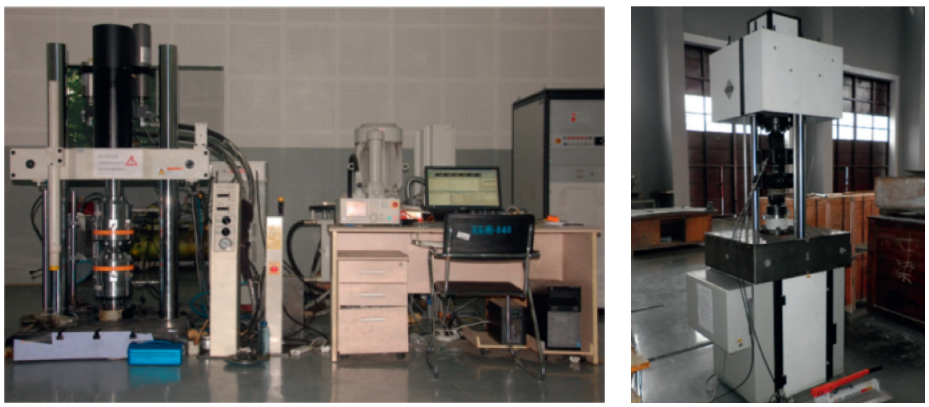

(a) (b)

Figure 15: Electrohydraulic servo high-frequency fatigue testing machine (Shimadzu).

In the experiment, there is a pause every 50,000 cycles to observe the weld damage of the specimens. The test will stop when crack initiation occurs at the weld. The fatigue test results are shown in Table 1.

3.3. S-N Curve of Fatigue Life. Assuming that the relationship between stress amplitude S and fatigue life N can be represented by a double logarithmic linear model,

$$\lg S = -\frac{1}{m}\lg N + \frac{1}{m}\lg C, \tag{2}$$

where C and m are the parameters determined by fatigue tests by using the least squares method. According to test results listed in Table 1, the fatigue life of the Q345 weldment can be estimated by

$$\lg S = -0.079\lg N + 2.620, \tag{3}$$

and Figure 17 shows the relationships between stress amplitude and fatigue life of Q345 welded specimens under the investigated loading conditions.

4. Effect of Residual Stress on Wind-Induced Fatigue Life of Weld Joint

4.1. "Welding-Wind-Induced" Response Characteristics at Welding Fatigue Critical Point. The equivalent stress time histories at the critical point of the welds for fatigue are shown in Figure 13 for the three cases: (1) the wind-induced stress time history without considering the effects of welding residual stresses (the bottom curve); (2) simply superposition of the wind-induced stress time history and welding residual stress (the top curve); (3) real stress time history of wind-induced stresses considering relaxation effect of the welding residual stresses, i.e., the "welding-wind-induced" response (the middle curve). It can be seen that due to the existence of welding residual stresses, the stresses at the critical point of the welds is much higher than that when the welding residual stress field is totally ignored. It can also be seen that if the welding residual stresses were simply superimposed to the wind-induced stresses, the resulting stresses would be higher than the yield stress, which unrealistically overestimates the stress responses and is completely inconsistent with the actual situation. If the coupling effect of wind-induced response and welding residual stresses is taken into account, that is, the relaxation effect of residual stresses is considered, the stress at the critical point of the welds is close to but lower than the yield stress steel and the welds of the welded joint may fail due to high cyclic stress fatigue at the welds under wind loading.

Compared with "wind-induced" stress, the "welding-wind-induced" stress at the critical point has the following characteristics: (1) The average stress level of the "welding-wind-induced" stress time history curve should increase considerably, and it can approach (but not exceed) the yield strength of structural steel. For the curves shown in Figure 18, the mean value of the equivalent stress is 122.8 MPa for the "wind-induced" case and 275.6 MPa for the "welding-wind-induced" case. (2) The peak-to-peak value of the "welding-wind-induced" stress time history curve should be reduced greatly.

Table 1: Fatigue test results.

Stress amplitude S (MPa)		220	200	175	162.5	150	137.5	125
Cycles to failure N	1st group	20904	52365	153986	408972	1096349	1449875	3386537
	2nd group	11291	65401	135922	387740	1144660	1561927	2784066

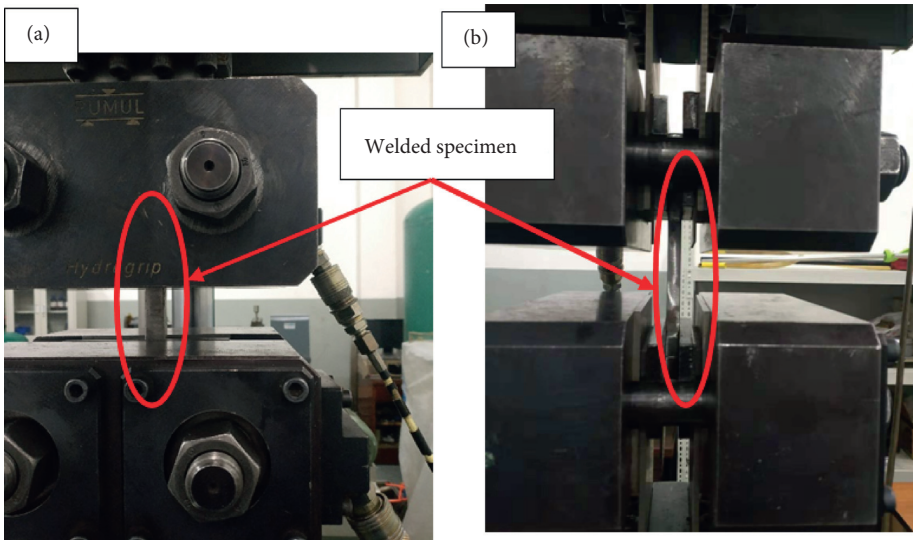

Figure 16: The installation of the welded specimens. (a) Front face; (b) side face.

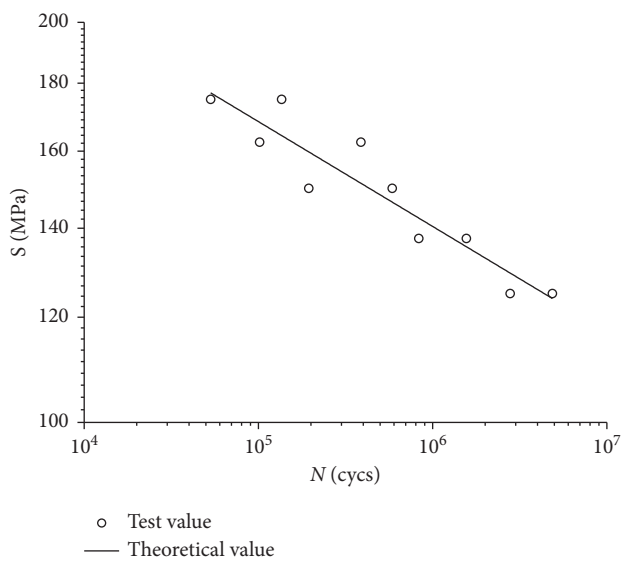

Figure 17: Relationship of stress amplitude versus fatigue life of welded specimens.

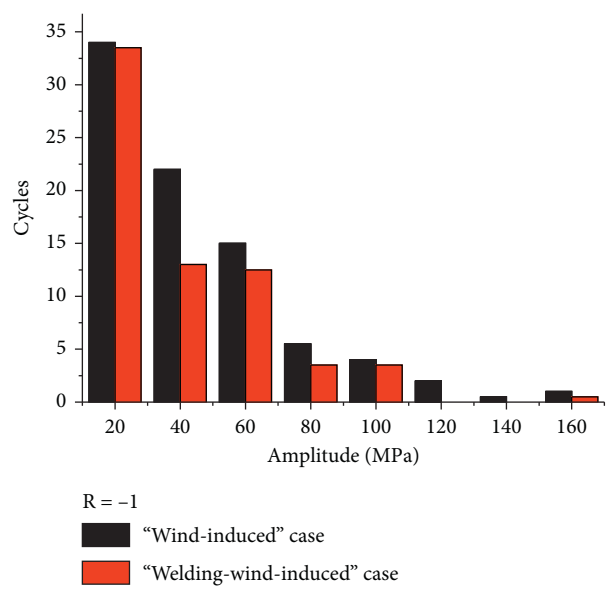

Figure 18: Histogram of stress amplitudes.

4.2. Fatigue Damage Calculation at Critical Points of Welded Joints. Figure 13 demonstrates that, when the effect of welding residual stress is considered, the average stress at the fatigue critical point of the welded joint increases, while the stress amplitude decreases. According to the fatigue theory of metal material [22], the former will increase fatigue damage and shorten the fatigue life, while the latter will mitigate fatigue damage and prolong the fatigue life. Therefore, the total influence of residual stress on fatigue life depends on the combined effect of these two factors.

As discussed in Section 2.5, the three-dimensional stress states of the welded joint can be regarded as in-phase loading. Therefore, based on the S-N curve of stress fatigue life for the welded specimens, the high-cycle multiaxial fatigue life of key welded joints can be estimated by the von Mises criterion and the Miner linear fatigue cumulative damage theory.

Since the experimental S-N curve of fatigue life of Q345 steel weldment is obtained by cyclic stress with zero mean value, the equivalent stress response shown in Figure 13 of

the welded joint with nonzero mean value should be corrected based on the Goodman equation [22] as

$$\frac{S_a}{S_{-1}} + \frac{S_m}{S_u} = 1,$$
$$S_{a(R=-1)} = \frac{S_u \cdot S_a}{S_u - S_m}, \tag{4}$$

where S_u is the fatigue limit of the material, the value measured by the test is 520 MPa; S_a is the cyclic stress amplitude; and S_m is the average stress.

Then the equivalent stress spectrum can be obtained by using the rain-flow counting method. The stress spectrum data are classified, and for each level of stress range, the counted actual number of cycles is given in Table 2 and Figure 18, respectively. It can be found that the number of cycles for the "welding-wind-induced" case decreases at all levels of stress range compared with that for the "wind-induced" case.

Finally, based on the Palmgren–Miner linear fatigue cumulative damage formula for cyclic stress with variable amplitude, the damage extent at the fatigue critical point of the welded joint can be obtained quantitatively by

$$D = \sum_{i=1}^{n} \frac{n_i}{N_{\mathrm{fi}}}, \tag{5}$$

where D is the cumulative fatigue damage value and n_{i} and N_{fi} are the number of cycles accumulated and corresponding fatigue life at the ith cyclic stress σ_i. $D = 1$ means the occurrence of fatigue failure.

For the along-wind-induced stress response with the duration of 100 seconds as shown in Figure 13, the fatigue damage values at the critical point of the welded joint are listed in Table 3. Correspondingly, the fatigue crack initiation lives at the critical points of welded joints in guyed mast are also given in Table 3.

It is interesting that welding residual stress can decrease fatigue damage and extend fatigue life of weld joints of guyed mast structure under the excitation of along-wind load. The fatigue life increased from 54.85 years to 96.60 years with an increase rate of about 76%. Obviously, in the two effects caused by welding residual stress on stress state at the fatigue critical point, the reduction of stress amplitude predominates fatigue life of the welded joint of the guyed mast.

5. Conclusions

This paper investigated effects of welding residual stress on along-wind-induced stress at the fatigue critical point of the welded joint in the guyed mast. The following conclusions can be obtained:

(1) The three-dimensional stress field of the welded joint of the guyed mast can be approximately considered as to be multiaxial proportional, and the stress-based von Mises criterion can be used to predict the high-cycle fatigue life of the welded joint.

Table 2: Classification data of the stress spectrum.

Stress amplitude S (MPa)		20	40	60	80	100	120	140	160
Cycles	"Wind-induced" case	34	22	15	5.5	4	2	0.5	1
	"Welding-wind-induced" case	33.5	13	12.5	3.5	3.5	0	0	0.5

Table 3: Fatigue damage value and fatigue life at critical points.

	Fatigue damage value in 100 seconds	Fatigue life
"Wind-induced" case	$5.78E-08$	54.85 year
"Welding-wind-induced" case	$3.28E-08$	96.60 year

(2) The welding residual stress can produce two effects on the equivalent stress time history at the fatigue critical point, that is, to increase average stress (near the yield strength but not beyond its level) and to reduce stress amplitude.

(3) The welding residual stress can increase fatigue life of crack initiation of the welded joint, in which the reduction of stress amplitude plays a key role. As far as the examples in this paper are concerned, the fatigue crack initiation life of the dangerous point is increased by about 76% after considering the welding residual stress.

Data Availability

The data used to support the findings of this study are available from the corresponding author upon request.

Conflicts of Interest

The authors declare that they have no conflicts of interest.

References

[1] P. H. Wirsching and A. M. Shehata, "Fatigue under wide band random stresses using the rain-flow method," *Journal of Engineering Materials and Technology*, vol. 99, no. 3, pp. 205–211, 1977.

[2] U. Peil and G. Telljohann, "Fatigue of high and slender structures under wind load," *Aspects in Modern Computational Structural Analysis*, pp. 77–83, Johns Hopkins University, Baltimore, MD, USA, 1997.

[3] R. Tovo, "Cycle distribution and fatigue damage under broad-band random loading," *International Journal of Fatigue*, vol. 24, no. 11, pp. 1137–1147, 2002.

[4] M. P. Repetto and G. Solari, "Wind-induced fatigue of structures under neutral and non-neutral atmospheric conditions," *Journal of Wind Engineering and Industrial Aerodynamics*, vol. 95, no. 9–11, pp. 1364–1383, 2007.

[5] C. S. Horas, J. A. F. O. Correia, A. M. P. De Jesus, P. Kripakaran, and R. Calçada, "Application of the modal superposition technique combined with analytical elasto-plastic approaches to assess the fatigue crack initiation on

structural components," *Engineering Fracture Mechanics*, vol. 185, pp. 271–283, 2017.

[6] H. He, H. Liu, C. Zhu, P. Wei, and Z. Sun, "Study of rolling contact fatigue behavior of a wind turbine gear based on damage-coupled elastic-plastic model," *International Journal of Mechanical Sciences*, vol. 141, pp. 512–519, 2018.

[7] L. Ziegler, S. Schafhirt, M. Scheu, and M. Muskulus, "Effect of load sequence and weather seasonality on fatigue crack growth for monopile-based offshore wind turbines," *Energy Procedia*, vol. 94, pp. 115–123, 2016.

[8] S. Lecheb, A. Nour, A. Chellil, H. Mechakra, H. Ghanem, and H. Kebir, "Dynamic prediction fatigue life of composite wind turbine blade," *Steel and Composite Structures*, vol. 18, no. 3, pp. 673–691, 2015.

[9] Y. Wang and C. Soutis, "Fatigue behaviour of composite T-joints in wind turbine blade applications," *Applied Composite Materials*, vol. 24, no. 2, pp. 461–475, 2017.

[10] Z. Fang, A. Li, W. Li, and S. Shen, "Wind-induced fatigue analysis of high-rise steel structures using equivalent structural stress method," *Applied Sciences*, vol. 7, no. 1, p. 71, 2017.

[11] S. A. R. Hosseiny and J. Jakobsen, "Local fatigue behavior in tapered areas of large offshore wind turbine blades," *IOP Conference Series: Materials Science and Engineering*, vol. 139, no. 1, pp. 12–22, 2016.

[12] T. Q. Do, H. Mahmoud, and J. Van De Lindt, "Fatigue life of wind turbine tower bases throughout Colorado," *Journal of Performance of Constructed Facilities*, vol. 29, no. 4, pp. 104–109, 2014.

[13] M. Shuang and B. Song, "Reliability analysis of wind turbines under non-Gaussian wind load," *The Structural Design of Tall and Special Buildings*, vol. 27, no. 3, Article ID e1443, 2018.

[14] P. Colombi and K. Doliński, "Fatigue lifetime of welded joints under random loading: rainflow cycle vs. cycle sequence method," *Probabilistic Engineering Mechanics*, vol. 16, no. 1, pp. 61–71, 2001.

[15] D. F. Socie and G. B. Marquis, *Multiaxial Fatigue*, SAE International, Warrendale, PA, USA, 2000.

[16] A. Fatemi and D. F. Socie, "A critical plane approach to multiaxial fatigue damage including out-of-phase loading," *Fatigue & Fracture of Engineering Materials and Structures*, vol. 11, no. 3, pp. 149–165, 1988.

[17] D. G. Shang and D. J. Wang, "A new multiaxial fatigue damage model based on the critical plane approach," *International Journal of Fatigue*, vol. 20, no. 3, pp. 241–245, 1998.

[18] J. Li, Z.-P. Zhang, Q. Sun, and C.-W. Li, "Multiaxial fatigue life prediction for various metallic materials based on the critical plane approach," *International Journal of Fatigue*, vol. 33, no. 2, pp. 90–101, 2011.

[19] M. Bäckström and G. Marquis, "A review of multiaxial fatigue of weldments: experimental results, design code and critical plane approaches," *Fatigue*, vol. 24, no. 5, pp. 279–291, 2001.

[20] D. Radaj, C. Sonsino, and W. Fricke, *Fatigue Assessment of Welded Joints by Local Approaches*, CRC Press, Boca Raton, FL, USA, 2nd edition, 2006.

[21] W. L. Qu, E. N. Zhao, and Q. Zhou, "Refined analysis of fatigue crack initiation life of beam-to-column welded connections of steel frame under strong earthquake," *Shock and Vibration*, vol. 2017, Article ID 7946286, 13 pages, 2017.

[22] C. Y. Chen, *Fatigue and Fracture*, Huazhong University of Science and Technology Press, Wuhan, China, 2002, in Chinese.